Simulated studies of water vapour tomography

PEEP MIIDLA
Institute of Mathematics,
University of Tartu
Liivi 2, 50409 Tartu,
ESTONIA
Peep.Miidla@ut.ee

KALEV RANNAT
Institute of Cybernetics
Tallinn University of Technology
Akadeemia 21, 12618 Tallinn
ESTONIA
rannat@cs.ioc.ee

PEEP UBA
Estonian National Defence
College
Riia 12, 51013 Tartu,
ESTONIA
peep.uba@ksk.edu.ee

Abstract: The technical success and availability of numerical algorithms have promoted the implementation of tomography to atmospheric sciences. The principal specific character in initial constraints, data collection and assimilation methods, obtaining the final numerical results and interpretation of these makes the continuation of the success story for GPS-tomography very challenging. Numerical simulation is the most time- and money efficient way to study different processes connected with tropospheric water vapour tomography. This paper gives a short overview of some mathematical methods for detection, monitoring and modeling of tropospheric water vapour. The possible mathematical approach to constructing a virtual ground-based sensors (GPS-receivers) network for a real geographical location and discretisation of the troposphere, also some aspects of raw data filtering and analysis are described. The outcome of tomographical modeling of the troposphere might to be applied to improve the results of large scale numerical weather prediction models. The questions of voxel geometry and methods of data processing are expected to be key questions in constructing an effective GPS-receiver network for water vapour tomography.

Key-Words: Global Satellite Navigation System, Troposphere water vapour, GPS-tomography, Kalman filter.

1 Introduction

The GNSS (Global Satellite Navigation System) with known realisations such as GPS, GLONASS and the forthcoming GALILEO has become a part of everyday life. The GPS-signal for positioning is particularly used to obtain information on the concentration of tropospheric water vapour as one of the most important of greenhouse gases and a carrier of latent heat in the atmosphere. Data about the distribution of water vapour also supports numerical weather prediction (NWP) models. Related large-scale experiments and monitoring have been launched in Japan (GEONET), US (SuomiNet), Europe (E-GVAP), etc.

Tomographic methods have been developed to get a 3D distribution of water vapour in the troposphere ([5],[10],[13],[20]). The work on improvement and efficiency of tomographic methods, depending on experimental setup and mathematical algorithms is an area of interest and a subject of investigations for many research groups.

The basic differences between medical and tropospheric tomography consist of the initial setup of measurements and the behaviour and nature of the detectable environment. In medicine we have an exact dense constellation of signal transmitters and receivers and full control of the movement of the test body. In the case of the troposphere one cannot control movements in the environment and the transmitter/receiver (GPS-satellite /GPS- receiver) constellation is variable and sparse. Even if the positions of the GPS-satellites are known in principal the real position is affected by orbital perturbations and the availability of precise orbits from the IGS-service is delayed. The new signal transmitters (the forthcoming GALILEO) and new frequencies will help to provide spatially more dense information from the atmosphere and to improve signal processing.

2 Water vapour tomography – How does it work?

GPS signals propagating from GPS satellites to receivers on the ground are affected by the atmosphere. The scheme of the receivers and satellites network is shown on the Figure 1. The 1-band receivers need to be supported by 2-band receivers (GPS3 on Fig. 1) to get information on ionospheric refraction as described below.

Figure 2 explains briefly how the presence of water vapour in the atmosphere can play a role of unwanted noise and from another hand, can be used as useful information for tomographic model and potentially as complimentary data input to NWP. One product of the tomography model can be an archive of IPW data at the site of measurements to detect climatological trends and their impact on nature. Climate change has a direct impact on vegetation [4].

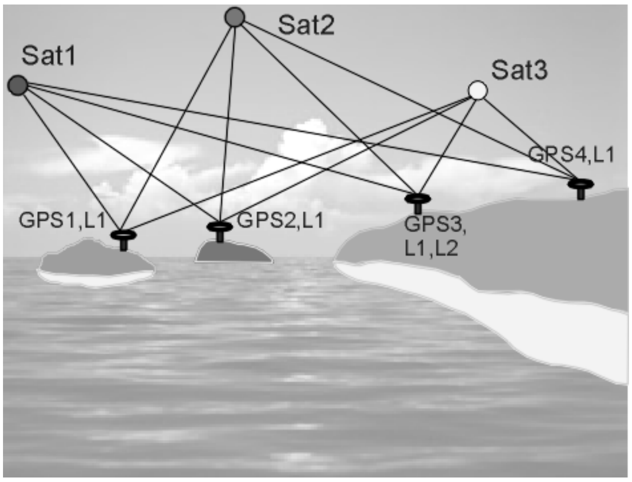

Figure 1. GPS receivers network.

Atmospheric refraction induces *slant delays* in individual rays propagating from GPS satellites to ground-based receivers. Slant delay is expressed by the excess path length of GPS radio signals along their propagation path between a GPS satellite and a ground-based receiver. The ionosphere has a dispersive effect on GPS-frequencies (L1=1575.42 MHz, L2=1227.60 MHz), while the troposphere has a non-dispersive effect on the GPS-signal. This allows the ionospheric effects to be removed by a linear combination of dual frequency measurements ([16],[18],[35]), the tropospheric impact cannot be determined by using 2-frequency techniques.

In general, the effect of both the ionosphere and troposphere can be measured by the additional delays of signal propagation on the receiver-satellite path. Due to atmospheric refraction the signal path is not the shortest straight line between receiver and satellite, but a form of curve (Fig. 3).

On the path to the receiver, different components of a GPS-signal will arrive at the antenna at a different instant of time. Ionospheric refraction causes a delay of the information package (modulated on the carrier signal) and the advance of the carrier phase. The physical reason for this is that the wave group- and phase speed depend on the refraction index of the environment. The analysis, determination and elimination of ionospheric effects are beyond the scope of this article. A more detailed description can be found from ([16],[18],[35]).

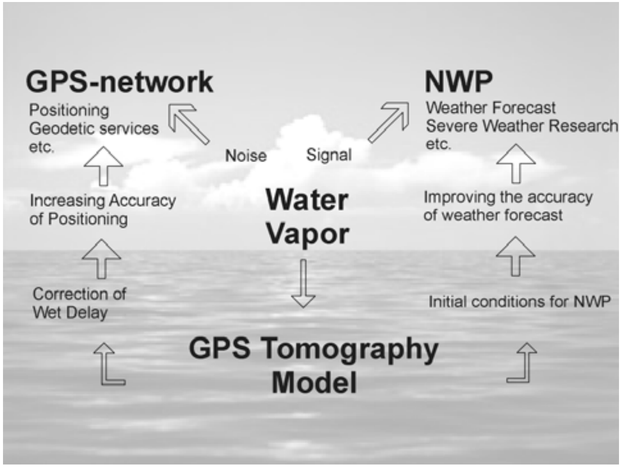

Figure 2**.** Getting the needed meteorological information from GPS navigation data.

The ionospheric delay can be removed (in the case of the model by adding supporting 2-band receivers to the monitoring network and the interpolation of the ionospheric constituents between grid points).

Molecules of tropospheric gases and hydrometeors have a negative effect on signal propagation: increasing the noise component in the GPS-receiver and absorbing the signal. In most cases this absorption is not a problem for GPS-networks. Atmospheric attenuation at GPS frequencies is in the order of 0.035 dB for a satellite at zenith and around 10 times more at low elevation angles. This attenuation is mostly caused by oxygen. The effects of water vapour, rain and nitrogen are negligible. Even dense rainfall causes attenuation of less than 0.01 dB/km [24].

The delay caused by neutral atmosphere can be separated into two components: a zenith hydrostatic delay (“dry” component, ZHD) as a result of the induced dipole moment and a zenith wet delay (“wet” component, ZWD) due to the permanent dipole moment of PW (Precipitable Water, water molecule) and liquid water (LW) present in the troposphere [27]. The wet component is spatially and temporally variable, therefore the errors in models for the wet component are larger than the errors in the models for the “dry”.

3 Slant Total Delay model

Although as yet not so widely used, the tomographic method based on Slant Total Delay (STD) [33] has several essential advantages compared to traditional integrated precipitable water (IPW) estimation, based on the Zenith Total Delay (ZTD) approach [25]. For high-resolution NWP the benefit of using STD comes from three main aspects: (i) the larger volume of observations available, as there are several satellites simultaneously visible and tomographically usable from each point of observation; (ii) STD-observations can contain information on atmospheric anisotropy - the gradients of temperature and humidity, while ZTD observations assume isotropic atmosphere; (iii) ZTD can be considered as a special case of STD, in other words, ZTD is derived from raw measurements along the slanted signal paths [9].

STD observations provide the potential for water vapour tomography – to obtain the real 3D distribution of tropospheric water for kilometric scale modeling, but on the other hand, the procedure for the production of STD observations is still in a stage of evolution. It is not convincingly clear if the accuracy of near real time STD observations is adequate for the operational demands of NWP systems. Due to the geometry of the slanted signal paths, assimilation of STD is not as straightforward as the assimilation of ZTD. Moreover, currently it is not known how to properly account for the complicated observation error correlations of STD ([8],[9]).

From the NWP point of view, ZTD is a desirable observation since it is a linear function of IPW above the GPS receiver [1]. IPW is directly related to the model humidity variable and it is ideally suited to the model geometry. The relative complexity of usage of slanted signal paths and the common practice of the NWP side has somehow suppressed the usage of water vapour tomography at an operational level. This gives all the more challenges for future research and modeling.

In fact the GPS-tomographic network does not need to be seen as an alternative to existing meteorological systems but something complimentary to it. GPS-based system can already detect water vapour and local extreme concentrations before any radar detection is possible. In this sense the GPS-tomographic system can serve as a warning system.

To study the methods and large-scale experimental setups, simulation is the most time- and cost effective way. The situation is modeled where information on water vapour content surveillance is obtained from ground-based GPS-receivers supported by additional meteorological sensors. Those can be considered as stand-alone proactive agents with individual environment-dependent inputs and outputs. The IPW from fixed geographical positions are obtained by using GAMIT/GLOBK software [15] and used as links between simulation and reality. Real data from fixed points is essential for the calibration and evaluation of the model.

Kalman Filtering (KF) (and its modifications) has been investigated as a means to minimize noise in the initial data.

4 The impact of the atmosphere

GPS signals propagating from GPS satellites to ground-based receivers are affected by atmospheric refraction. This induces *slant delays* which are manifested by the excess path length of GPS radio signals (Fig 3).

Ionospheric refraction causes a delay of the information package, modulated on the carrier signal and the advance of carrier phase. The physical reason for this is that the wave group- and phase speed depend on the refraction index of the environment.

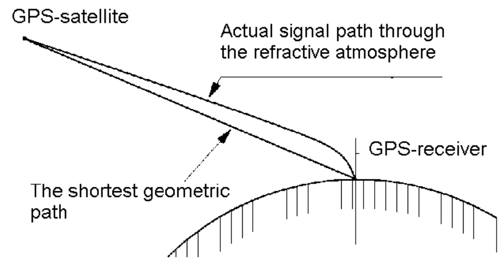

Figure 3. The signal path through the atmosphere.

The delay caused by neutral atmosphere can be separated into two components: a zenith hydrostatic delay ("dry" component, ZHD) as a result of the induced dipole moment and a zenith wet delay ("wet" component, ZWD) due to the permanent dipole moment of Precipitable Water and liquid water present in the troposphere [27]. The wet component is spatially and temporally variable, therefore the errors in models for the wet component are larger than the errors in models for the "dry".

STD is induced both by dry air and water vapour. Slant dry delay can be estimated from surface pressure measurements or from numerical weather models [6]. Slant wet delay (SWD) can be estimated as the difference between total slant delay and slant dry delay.

Tropospheric delay can be expressed as follows [16]:

$$\Delta^{trop} = 10^{-6}\int N^{trop} ds, \quad (1)$$

where $N^{trop} = 10^6(n-1)$ is often called a refraction and *n*(s) denotes the atmospheric refraction index on the signal path. Integration is performed over the total path in the troposphere.

Dividing the delay due to the tropospheric refraction into two components (*dry* and *wet*), the total delay can be expressed as

$$\Delta^{trop} = 10^{-6}\int N_d^{trop} ds + 10^{-6}\int N_w^{trop} ds. \quad (2)$$

This kind of dividing into components comes from practical considerations. The dry component of tropospheric delay is quite precisely described by different mathematical models (for example the models of Hopfield, Niell, Saastamoinen and others) [23]. Prediction and modeling of the wet component is complicated. The problem comes from the lack of measurement data and the instability of the troposphere (tropospheric turbulence).

Tropospheric refraction is often explained by empiric equations [16]:

$$N_{d,0}^{tropo} = \bar{c}_1 \frac{p}{T},\ N_{w,0}^{tropo} = \bar{c}_2 \frac{e}{T} + \bar{c}_3 \frac{e}{T^2}, \quad (3)$$

where $\bar{c}_1 = 77.64$ $K \cdot mb^{-1}$, $\bar{c}_2 = -12.96$ $K \cdot mb^{-1}$ and $\bar{c}_3 = 3.718 \cdot 10^5$ $K^2 \cdot mb^{-1}$, p is atmospheric pressure in mb, T is temperature in K and e is the partial pressure of water vapour. $\bar{c}_1, \bar{c}_2, \bar{c}_3$ are empiric constants. The results can be improved by measuring real meteorological data at the observation site. This should be a goal for any meteorological GPS-network, but usually meteo-data is interpolated from a point of measurement in an adjacent area. The measured data is entered into some of the known refractivity models. It is possible to get an estimate for the dry component of tropospheric delay $< 1mm$ if the pressure at the ground surface is measured with a precision of $0.3mb$ [7], but the wet component varies from some millimeters to 40 mm, depending on the latitude.

The amount of integrated water in the atmosphere in the zenith direction above the GPS-antenna is equivalent to the height of a column of liquid water. In a similar manner the slant water (SW) is defined, as the length of an equivalent column of liquid water on the ray path between GPS-receiver i and satellite m. SW_i^m is the Integrated Slant Water (ISW) vapour divided by the density ρ of liquid water $SW_i^m = ISW_i^m / \rho$, where

$$ISW_i^m = \int_{rec_i}^{sat_m} \rho_w ds \quad (4)$$

The ratio of SW to the Slant Water vapour Delay (SWD) is often known as a non-dimensional conversion factor Π, expressed as $\Pi = SW_i^m / SWD_i^m$. Here SWD_i^m can be derived from the STD measurements described in [9]. The IPW and SW can be easily found, as IPW=Π·ZWD and SW= Π·SWD (assuming the atmosphere is isotropic).

$\Pi \neq const$, depends on real environmental parameters [2], mostly on the mean temperature of the atmosphere, T_m, defined in ([27],[32]).

Water-vapour-weighted atmospheric mean temperature, T_m, is a key parameter in the retrieval of atmospheric precipitable water (PW) from ground-based GPS measurements of ZPD/SPD, as the accuracy of the GPS derived PW is proportional to the accuracy of T_m. The RMS (root mean square) error of GPS-derived PW ranges from smaller than 2 mm in North America to 3.7 mm in Japan. An uncertainty of 5 K in T_m corresponds to 1.6–2.1% uncertainty in PW. T_m has also temporal and spatial variations, described in [32].

For practical troposphere monitoring (for real reference data) the Trimble NetRS GPS-receiver was used at 58°23'30" N, 26°41'41" E, with an antenna height of 75.80 m above the reference ellipsoid. The data has been captured from December 2006 onwards. The data post-processing is performed by GAMIT.

GAMIT-processing helps to obtain the real path and delay of the signal from each satellite to the receiver. The difference between real and – geometrical gives the initial information needed for tropospheric water estimation. GAMIT software uses the Global Mapping Function by default, as developed by Boehm et al. [3] for atmospheric delays calculation. In the absence of *in situ* meteodata, the best choice of *a priori* pressure and temperature for a site comes from the global pressure and temperature (GPT) model [15].

In Figure 4 a 54 day period is represented by the corresponding evolution of Integrated Precipitable Water, temperature, relative humidity and air pressure in Tartu.

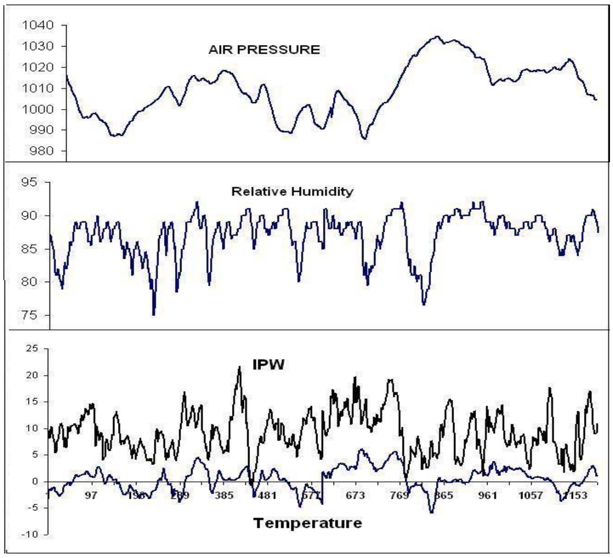

Figure 4: Pressure, relative humidity, precipitable water and temperature in 06. Nov - 29. Dec. 2007. Horizontal resolution 1 hr.

The presented results are un-smoothed. The short-term evolution of relative humidity at ground level and the IPW are quite unstable. It can be interpreted as atmospheric turbulence, but the result also contains all possible discrepancies at this stage.

5 Error management and numerical filtering of the initial data

Although GPS-measurements are believed to be extremely accurate for nearly every application, they can exhibit significant errors depending on environmental conditions and the technical setup of experiments. From the modeling point of view and for geodetic accuracies the results are mostly affected by orbit errors and clocks drift.

Assimilation of the results into NWP models needs accuracies of better than 2 mm of PWV (Precipitable Water Vapour) within 1 h of data collection [14]. For now-casting (often referred as the forecasting of the weather in the 0-12 hrs timeframe) the TOUGH project report [30] recommends a time resolution of nearly real time (NRT) GPS data as high as 2-4 observations/hour with an update every hour, with a potential for faster updates in the future.

The first obstacle for geodetic data processing is related to the delayed availability of precise orbits of GPS-satellites. For real- and near real time applications only predicted or Ultra Rapid products can be used. Improvement can be achieved by using the sliding-window technique (e.g. [11]).

The orbits errors are systematic (except on the occasions of Sun bursts), therefore they are easier to handle. The receiver clock errors can be mostly eliminated by the double-differencing method. The systematic errors can be eliminated by combining and comparing different data from observations.

Atmospheric tomography (and the related modeling) has additionally some specific sources of errors, which are impossible to ignore. The *first* is related to voxels (the meaning of the term is presented later), not giving any information because of not being intercepted by any signal ray. The *second* is related to real data acquisition at the point of measurement - sudden malfunction of some of the sensors or loss of the data.

The *first* category of problems is expected to be smoothed by Kalman Filtering (KF). KF and smoothing have also been used in the GPS-campaign at Onsala, described in [10]. The successful exploitation of KF or its modifications ([17],[19],[34]) is not always straightforward due to limitations emanating from the receiver's network geometry. KF also needs observability and controllability conditions to be satisfied [12], otherwise the algorithm will not converge. One possibility to overcome the geometry limitations is by exploiting the Wet Refractivity Kalman Filter [13].

The *second* category of errors is overcome by using the paradigm of *agents*. In this concept each node of the GPS-receivers network is considered to be an autonomous proactive agent, with the main task of capturing the data on GPS-observations and 3 additional meteo-parameters. Additionally, each node (agent) is responsible on the data link to a central data processing unit. If for example one meteoparameter (let's say ground surface temperature) is missing, then it can be requested from adjacent agents, the result being interpolated for the malfunctioning node and the "complete" data sent to the central unit. This makes it technically possible to distribute some operational tasks to the agents in the nodes leaving the more computational resources to the data processing unit.

Random measurement errors are also processed by KF. KF addresses the general problem of trying to estimate the state X of a discrete-time controlled process that is governed by the linear equation on its development from the time point k-1 to the instant k:

$$X_k = AX_{k-1} + w_{k-1}. \qquad (5)$$

Assume also that the measurement Z is expressed by the state vector X:

$$Z_k = HX_k + v_k. \qquad (6)$$

Here X and Z are the vectors of n- and m-dimensional real Euclidean space respectively. The random variables w_k and v_k represent the process and measurement of noise (respectively). They are assumed to be independent of each other and auto-independent, while, with normal probability distributions. In practice, the process noise covariance and measurement of noise covariance matrices Q and R might change at each time step, however here are assumed constant. The $n \times n$ matrix A in the equation (5) relates theoretically to the state at the previous time step $k-1$ to the state at the current time step k, in the absence of either a driving function or process noise. Note that in practice A and H might change with each time step, but here we assume those are constant matrices. The $m \times n$ matrix H in the measurement equation (6) relates the state to the measurement Z_k .

Finding the best modification of KF is one of the next challenges for modeling, as numerical precision and stability is counterbalanced with computational load, directly related to the applicability of the monitoring concept and surveillance network.

One important aim in obtaining information about water vapour distribution in the troposphere is to use the results as input for large-scale NWP models. The output introduced from GPS-tomography is the concentrations of water vapour in every single voxel. This means that observers have a set of virtual humidity sensors covering the whole area under consideration. These are on one hand moving dynamically and for some parts of the troposphere (for some voxels) may be interpolated, but also on the other hand, do not need service and do not disturb aviation. The obtained information used as feedback for a better estimation of the state of weather is made possible through KF.

6 GPS-receivers network and discretization of the troposphere

The installation of the GPS-receivers network for tropospheric tomography is modeled. Tomographic methods to obtain the 3D distribution of tropospheric water have been a subject for numerous investigations ([5],[10],[13],[20]).

The initial idea comes from conventional tomography, known in medicine. The information on ray propagation (delaying or attenuation) in a certain part of environment is obtained from different angles and later the image of the investigated constituents is reconstructed by tomographic algorithms. In medicine the 3D image is obtained by signals coming from all available directions while in tropospheric tomography we get all the observations between the top layer and the ground only. In the model situation the delay is equivalent to the signal path (additional delay corresponds to the prolongation of the path).

From the atmospheric point of view the GPS-signal time delays and the contributions of atmospheric water to the delays in every discrete part of the troposphere (hereafter called *voxel*) are under consideration. The discretization of the troposphere into rectangular voxels is explained in Figure 5. Different geometrical setups exist for building the voxel system, but for the simulation experiment a rectangular grid is chosen for simplicity (assuming the monitoring area is relatively small).

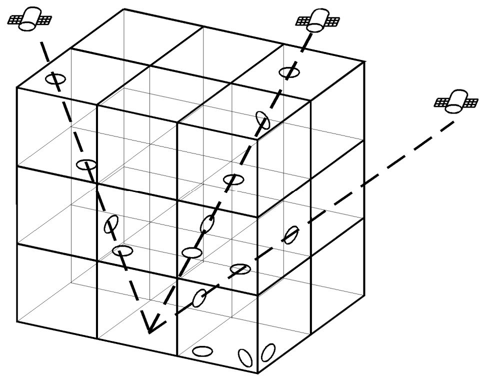

Figure 5. Ray paths from the satellites to a GPS-receiver through rectangular voxels.

There is very little information available regarding the voxel system. In general the geometry of the tomographic system will stay weak. The situation is improved a little when taking the Earth’s curvature into account (Figure 6). The latter cannot be ignored for large-scale tomography, for areas of some hundreds of quadratic kilometers.

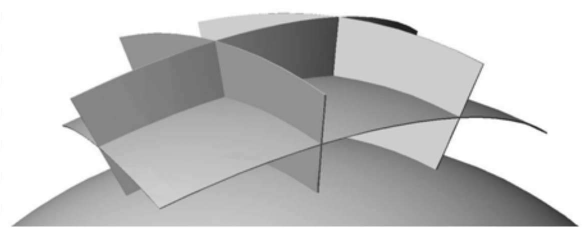

Figure 6. Curved voxels.

The voxel boundaries are constructed on a spherical system of coordinates [26]. Orthogonal Earth-centered coordinates (x,y,z) and spherical coordinates (ρ,φ,λ) are mutually transformed by formulas x = ρ cosφ sinλ ; y = ρ sinφ sinλ ; z = ρ cosλ .

Attempts to obtain improvement are also being made with irregular grids [21]. Probably a "best solution" for a geometrical setup does not exist. Every local network should be studied and modeled case by case. Surface relief also has to play an important role. It would be ideal if the measurement points could reside in every layer of the voxel system. The Swiss AGNES network for example has height differences ca 3000 m between the highest and the lowest station, but even then only 2 stations are situated above 2000 m [28]. Unfortunately natural height differences are not the case in Estonia and other relatively flat areas.

Below we consider the rectangular voxel system. Tropospheric water is mostly distributed in a layer with a thickness of up to 7 – 10 km. The horizontal resolution 10-40 km of the grid is usually taken in similar experiments (station separations ~50 km or less are recommended in the final report of the TOUGH-project [29]). Similar grid-steps are used also in other fields of atmospheric modeling [22,31]. Detecting water vapour takes into account all the GPS-signal ray paths (where the signal has a high enough quality) from the visible satellites into each location of GPS-receivers. The maximum number of ray paths is $n \cdot m$, where n corresponds to the number of satellites and m to the number of receivers. Hereby it must be noticed that n corresponds to a number of those satellites only that can be technically used in the experiment (having acceptable signal/noise ratio at a point of observation). This means that n can be smaller than the number of visible satellites and additionally, the number of usable ray paths can be reduced due to technical conditions.

The bottom facet of the voxel is rectangular. The parameters for construction of the voxel system are the size of the horizontal grid (distance between the receivers) and each vertical step (corresponding to a number of layers in the model troposphere). The bottom of the voxel system is a tangent plane at a geographical point to the Earth as an ellipsoid. This geographical point serves as the middle point of the simulation area (middle of the virtual GPS-network).

Figure 7 demonstrates one of the simulated situations with a certain constellation of satellites, their positions related to the voxels. 144 voxels were chosen for the simulation and placed on six horizontal levels (24 voxels in each). The receivers were placed into each voxel on the ground surface, with a total number of 24. With 11 visible GPS-satellites this gives a system of 264 equations for 144 unknowns.

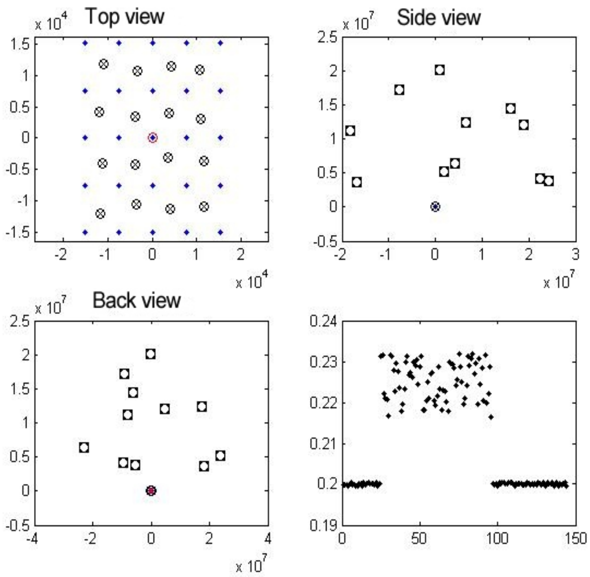

Figure 7. Positions of the satellites and receivers over the area of simulated experiment and the possible prolongation of the path in voxels.

In the upper row and in the left hand image of the lower row, circles with crosses denote the positions of GPS-receivers, the square panels with a circle in the middle denote the positions of satellites and the squared dots denote the vertexes of voxels. The right hand panel on the lower row explains the graphical image of the solution of the model system (the delays of signals in voxels).

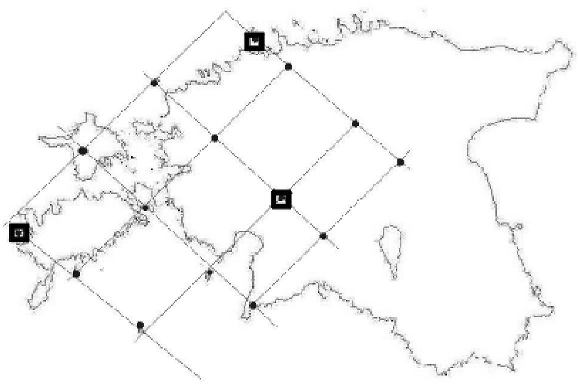

Figure 8. Hypothetical GPS receivers network in Estonia.

The Figure 8 shows the possible GPS-receivers network configuration in Estonia for real water vapour monitoring in the area.

7 The model

Each signal on the path between a receiver and the satellite penetrates a certain number of voxels. Each voxel (with water vapour) makes its individual contribution to the total delay of the signal corresponding to Eq. (3). The full path of the signal is a sum of the paths in the intercepted voxels. The model can be interpreted as a system of linear equations

$$\sum_{i=1}^{v} x_i \cdot s_{i,j} = f_j, \tag{8}$$

where j = 1,…, K, K is the total number of signal paths from all visible satellites in the GPS-network at a fixed instant in time, v is the total number of voxels, $s_{i,j}$ is the length of the j[th] ray in voxel i, the x_i are considered as weights of a voxel corresponding to the slant path delay and interpreted as indicators of the PW concentration. Interpretation of the solution of the system of equations Eqs. (8) gives the distribution of water vapour by the voxels. The differences between the geometrical shortest path and the extra path, induced by tropospheric water (depending on the temperature, humidity and air pressure at the point of measurement), are specified by the absolute term f_i in an underdetermined system of linear equations (Eqs. 8). Based on the precise trajectories of the satellites (obtained from the IGS-service) the ray path length in each voxel is found, composing the system (Eqs. 8).

The system is resolved by the Least Squares (LS) method. It can be resolved also by Kalman Filter, using the prediction and correction step alternately.

The model software has two main tasks – (i) to construct the voxel system according to initial model parameters with the handling of voxel related data and (ii) the monitoring of the signal ray paths through the voxels. Hereby it should be mentioned that the model (also the GPS-receivers network) obtains the slant delays directly from the GPS signal phase observations, similar to the description in [20].

The geometrical shortest paths (Figure 1) are constructed from all satellites to all of the receivers according to the satellite constellation at a certain time instant. For each signal path the intercepted voxels will be found with geometrical points of ingoing and outgoing (to fix the shortest possible ray path inside the voxel). These partial lengths are used as coefficients in Eqs. (8). Each ray will penetrate only a minor part of voxels and the situation changes with each time step.

The simulation of monitoring consists of generation of initial data for a certain mathematical model and the data processing related to a specific scenario. The synthetic data consists of the outputs of GPS-receivers (including both (i) the data sent by a satellite and (ii) the data generated by a receiver).

The *first category* represents mostly the positions of the satellites, and the time parameters of atomic clocks. This data is consisted in a GPS-satellite’s navigation message and can also be obtained from GPS Ground Control Stations or some public databases via the internet. The *second category* consists of data about the time instants the signal was received (receiver time), carrier phase, the position of satellites (from receivers point of view) and some supporting information.

The simulation program, compiled on the basis of the mathematical model, is responsible for the generation of a situation that is as realistic as possible. The model situation must be described by a real geographical location and a real constellation of GPS-satellites at a certain time instant. Based on this information additional analysis is performed to find suitable locations for GPS-receivers in the monitoring network. The criterion is the solution of Eqs. (8) – the result must be realistic in a meteorological sense.

The simulation helps to specify in which initial conditions the system (Eqs. 8) can be resolved and when the result is reliable.

As a rule, the system of Eqs. (8) has less equations than unknowns (the number of signal rays is smaller than the number of voxels). Depending on the temporary constellation of GPS-satellites and receivers in the ground-based network, the system can be either unresolved or the solution is not precise enough (unrealistic). The results are also affected by the allocations of the receivers relative to each-other, the number of receivers and geographical position (regarding the constellation of satellites). Depending on the abovementioned reasons and the configuration of the voxel's system, the system of linear equations (Eqs. 8) can be over-, under- or normally determined.

Based on the analysis of different initial conditions and the solutions of model equations, it can be concluded – that the more homogeneous the GPS-receivers network is, the better the result. In fact, the reality is not so simple regarding the installation of the network — the sensors are installed in positions considering the practical possibilities. Simulation helps to find the best available spatial setup for the receiver’s network.

For ideal conditions the GPS-receivers need an open horizon and that is impossible to guarantee in

reality (the nearby forests, high buildings, etc. mask a certain part of the sky or initiate additional inaccuracy in measurements).
The moisture level per each voxel can be derived by interpreting the numeric solution of the model. In the simulation package this is done by a stand-alone module.

The amount of water vapour is found, using the delays in ([7], [8], [21]) voxels and the conversion factor Π. Information on all voxels gives a 3D distribution of water vapour in the troposphere and additionally IPW. The IPW can also be found from real measurements and GAMIT-processing at a certain point in the monitoring area (for the current experiment the station at 58°23'30" N, 26°41'41" E). This gives a possibility for validation of the model. As a favorable by-product from GAMIT-processing, the STD can be derived and compared to the total delays calculated by the simulation model. The temporal and geographical variation of Π is unknown, but using the estimated value around 0.15 satisfies the simulations at the current stage.

It is foreseen that the simulation will lead to the practical monitoring of tropospheric water. Based on the modeling results (the best geometry), the GPS-receivers network can be installed with the supporting meteorological sensors and data communication devices. A quite independent task will be the optimization of the communication network and protocols for real-time (or near real-time) application.

8 Conclusions

The modeling and simulation approach briefly described above, is the initial phase in developing a ground-based GPS-network for meteorological purposes by the authors. Collaboration can be foreseen with the Estonian Land Board and the Estonian Meteorological and Hydrological Institute in establishing the common monitoring network and database, but also on international level.

The modeling environment works well for receiver-network geometry analysis. The concept of agents helps to model situations closer to reality and to decentralize the data processing load. The future effort is targeted on data filtering as it is not clear what kind of KF will give the best result and how to resolve the questions of poor voxel geometry in an optimal way. These two topics will probably be the key questions in constructing an effective GPS-receiver network for water vapour tomography.

This paper is supported by the grant No. 7097 of Estonian Science Foundation.

References:

[1] Bevis, M., S. Businger, T. A. Herring, C. Rocken, R. A. Anthes, and R. H. Ware. GPS meteorology: Remote sensing of atmospheric water vapour using the Global Positioning System. *J. Geophys. Res.,*Vol. 97, 1992, pp 15,787-15, 801.

[2] Bevis, M., S. Businger, S. Chiswell, T. A. Herring, R. A. Anthes, C. Rocken, and R. H. Ware. GPS meteorology: Mapping zenith wet delays onto precipitable water. *J. Appl. Meteorol.,*Vol. 33, 1994, pp 379-386.

[3] Boehm, J., Niell, A., Tregoning, P., Schuh, H. Global Mapping Function (GMF): A new empirical mapping function based on numerical weather model data, *Geophysical Research Letters*, Vol. 33, 2006, L07304, doi:10.1029/2005GL025546.

[4] Boonklong, O., Jaroensutasinee, M., Jaroensuta sinee, K. Effects of Climate Change on Mangosteen Production in Thailand, WSEAS Transactions on Environment and Development, 9, vol. 2, Sept. 2006, pp. 1291.

[5] Braun, J.J. and C. Rocken. Water vapour tomography within the planetary boundary layer using GPS. *Proceedings of the International Workshop on GPS Meteorology, GPS Meteorology: Ground-Based and Space-Borne Applications* (Tsukuba, Japan, January 14-17, 2003).

[6] Chen, G., and T. Herring, Effects of atmospheric azimuthal asymmetry on the analysis of space geodetic data." *J. Geophys. Res.*, Vol. 102, 1997, pp 20,489-20,502.

[7] Duan. J.P. and Coauthors, GPS Meteorology: Direct Estimation of the Absolute Value of Precipitable Water. *Journal of Applied Meteorology*, Vol.35, 1996, No.6, pp 830-838.

[8] Elosegui, P. Davis, J. Accuracy assessment of GPS slant-path determinations. In: *Proceedings of the International Workshop on GPS Meteorology*, Tsukuba, Japan, 14–17 Jan 2003 (eds. T. Iwabuchi and Y. Shoji).

[9] Eresmaa, R., Järvinen, H. An Observation operator for ground based GPS slant delays". *Tellus A*, 58, No 1, 2006, pp 131-140.

[10] Flores, A., L.P. Gradinarsky, P. Elosegui, G. Elgered, J.L. Davis and A. Rius. Sensing atmospheric structure: tropospheric tomographic results of the small-scale GPS campaign at the Onsala Space Observatory. *Earth Planets Space*, No. 52, 2000, pp 941-945.

[11] Foster, J., Bevis, M., Businger, GPS Meteorology: Sliding-Window Analysis. *Journal*

of Atmospheric and Oceanic Technology, AMS, Vol. 22, 2005, pp 687-695.

[12] Gelb, A. (ed.) Applied Optimal Estimation, MIT Press, Cambridge, MA., 1984.

[13] Gradinarsky, L.G**.** Sensing Atmospheric Water Vapour Using Radio Waves. PhD thesis, *Chalmers University of Technology*, *Technical report* No 436, 2002.

[14] Gutman, S.I., Benjamin, S.G. The role of ground-based GPS meteorological observations in numerical weather prediction. *GPS Solutions*, Vol. 4, 2001, pp 16-24.

[15] Herring, T. A., King, R. W., McClusky, S. C. *GAMIT Reference Manual*, Release 10.3, Department of Earth, Atmospheric, and Planetary Sciences, MIT, 2006.

[16] Hofmann-Wellenhof, B., H. Lichtenegger and J. Collins. *GPS Theory and Practice*, Springer-Verlag Wien, NewYork, NY, USA, fifth edition, 2001.

[17] Kalman, R.E., A new Approach to Linear Filtering and Prediction Problems". *Transaction of the ASME – J. of Basic Engineering*, March 1960, pp.35-45.

[18] Klobuchar, J., Ionospheric effects in GPS. In: B. Parkinson, J. Spilker (eds) *Global Positioning System: Theory and applications*, AIAA, Vol. 1, Chapter 12, 1996.

[19] Lange, A.A., Simultaneous Statistical Calibration of the GPS signal delay measurements with related meteorological data, *Physics and Chemistry of the Earth*, Part A: Solid Earth and Geodesy, Vol. 26, No. 6-8, 2001, pp 471-473.

[20] Nilsson, T**.,** Assessment of Tomographic Methods for Estimation of Atmospheric Water Vapour Using Ground-Based GPS. *Thesis for the degree of Licentiate of Engineering*. Chalmers University of Technology, 2005.

[21] Nilsson, T., Gradinarski, L. Water Vapour Tomography Using GPS Phase Observations: Simulation Results, IEEE Transactions on Geoscience and Remote Sensing, Vol.44, 10, Oct. 2006, pp. 2927-2941.

[22] San Jose R., Perez, J.L, Gonzalez, R. M., Air Quality CFD and Mesoscale Modeling Simulations: Madrid Case Study, WSEAS Transactions on Environment and Development, 10, vol. 2, Oct. 2006, pp. 1291.

[23] Shrestha, S.M., Investigations into the Estimation of Tropospheric Delay and Wet Refractivity Using GPS Measurements. *A Thesis in partial fulfillment of the requirements for the degree of Master of Science*. Calgary, Alberta, 2003.

[24] Spilker Jr., J.J. 1996. "Tropospheric effects on GPS" In: B. Parkinson, J. Spilker (eds) *Global Positioning System: Theory and applications*, Vol. I, Chapter 13.

[25] Stoew, B., Jarlemark, P., Johansson, J., Elgered, G., Real-time processing of GPS data delivered by SWEPOS. *Phys. Chem. Earth (A)* Vol. 26, 2001, pp 493–496.

[26] Tammo, P., Simulation of the output of GPS receiver (in Estonian). Bachelor thesis, University of Tartu, Institute of Applied Mathematics, 2007.

[27] Tregoning, P., Accuracy of absolute precipitable water vapour estimates from GPS observations. *Journal of Geophys. Res.*, Vol. 103, 1998, pp 28701-287109.

[28] Troller, M. GPS based Determination of the Integrated and Spatially Distributed Water Vapour in the Troposphere, Diss. ETH No. 15513, 2004.

[29] Vedel, H. et al. Final report for the TOUGH project". In: H. Vedel (Co-ordinator), *Targeting Optimal use of GPS Humidity Measurements in Meteorology*, EVG1-CT-2002-00080, 6th Periodic Report, 1 February 2003 – 31 January 2006, Section 6, http://tough.dmi.dk, (last visited 04.11.2007).

[30] Vedel, H. et al., GPS Data Recommendations for European Numerical Weather Prediction". In: H. Vedel (Co-ordinator), *Targeting Optimal use of GPS Humidity Measurements in Meteorology*, Deliverable D73, http://tough.dmi.dk, 2006 (last visited 04.11.2007).

[31] Vongmahadlek, C, Boonsong, S, Applicability of RAMS for A Simulation to Provide Inputs to an Air Quality Model: Modeling Evaluation and Sensitivity Test. WSEAS Transactions on Environment and Development, 8, vol. 3, Aug. 2007, pp. 129-138.

[32] Wang, J., Zhang, L., Dai, A., Global estimates of water-vapour-weighted mean temperature of the atmosphere for GPS applications. *Journal of Geophysical Research*, Vol. 110, 2005, D21101, doi:10.1029/2005JD006215

[33] Ware, R., C. Alber, C. Rocken, F. Solheim. 1997. "Sensing Integrated Water Vapour along GPS Ray Paths." *Geophys. Res. Lett.*, Vol. 24, 1997, pp 417-420.

[34] Welch, G., Bishop, G., *An Introduction to the Kalman Filter*. University of North Carolina. Shapel Hill, TR 95-41, 2003.

[35] Xu, G., GPS. *Theory, Algorithms and Applications*. Springer Verlag Berlin, Heidelberg, 2003.